Pergamon

PII: S0191-8141(96)00094-6

Journal of Structural Geology, Vol. 19, Nos 3–4, pp. 257 to 267, 1997

0191-8141/97 $17.00 + 0.00

Distribution of fault slip in outcrop-scale fault-related folds, Appalachian Mountains

DAVID A. McCONNELL, SIMON A. KATTENHORN* and LISA M. BENNER

Department of Geology, University of Akron, Akron, OH 44325-4101, U.S.A.

(*Received* 2 *February* 1996; *accepted in revised form* 8 *October* 1996)

Abstract—Current kinematic models of ramp-related folds predict a direct relationship between ramp angle and fold shape and imply specific sequences of deformation. Analyses of outcrop-scale structures in the Valley and Ridge province of the Appalachians reveal configurations that depart from model predictions. The models fail to account for the presence of footwall synclines, and are inconsistent with measured displacement distributions on some natural faults. Observations support the interpretation that faults can grow by propagation both up- and down-dip from a nucleation point. Fault propagation in either direction may result in the formation of folds primarily on the side of the fault that is displaced in the direction of fault propagation. © 1997 Elsevier Science Ltd. All rights reserved.

INTRODUCTION

Several geometric and kinematic models of fault-related folds have been developed in recent years as aids to structural interpretations of fold-and-thrust belts (Suppe, 1983; Suppe and Medwedeff, 1984, 1990; Jamison, 1987; Chester and Chester, 1990; Mitra, 1990; McNaught and Mitra, 1993; Wickham, 1995). Geometric models relate fold shapes with fault angles (or vice versa) for specific structures (Jamison, 1987). The primary role of these models is to generate a geometry that closely resembles that of a natural structure, regardless of the deformation history of the rocks. Kinematic models imply specific deformation sequences. Both geometric and kinematic models predict that fold shape is dependent, at least in part, upon fault geometry.

Suppe (1983) presented an elegant quantitative treatment that related fold shape to the geometry of thrust faults, and that made possible the construction of idealized balanced cross-sections through fault-bend folds (Fig. 1a). This technique has been widely applied to generate interpretations of subsurface structures (Mount *et al.*, 1989). Inherent in Suppe's kinematic model, and implied in many restored cross-sections that return the deformed structures to an 'undeformed' state, are the assumptions: (1) a flat-ramp-flat fault shape is present *prior* to slip on the fault or forms instantaneously at the moment slip is initiated; (2) the hanging wall is transported over a stationary footwall; (3) the footwall is undeformed; (4) fault displacement is uniform on hanging wall flats and decreases up-section across the hanging wall ramp (Fig. 1a).

Folds that form adjacent to the tips of thrust faults have been termed leading edge folds (Boyer, 1986) and tip anticlines (Mitra *et al.*, 1988). Possible kinematic relationships between thrust faults and folds have been modeled as fault-propagation folds (Suppe and Medwedeff, 1984, 1990; Chester and Chester, 1990), break-thrust folds (Fischer *et al.*, 1992), and fault displacement–gradient folds (Wickham, 1995). Fault-propagation folds grow as a thrust ramp propagates up-section from a bedding-parallel fault segment (Fig. 1b; Suppe and Medwedeff, 1984, 1990; Mitra, 1990). Some characteristics of these models are: (1) layers in the steep forelimb of the fold initially pass through an angular syncline hinge; (2) the hanging wall is transported over a stationary footwall; (3) footwall rocks are undeformed; (4) displacement decreases uniformly up-section on the ramp; (5) the ramp cuts up-section through the syncline hinge. Chester and Chester (1990) presented an alternative geometric model which assumed the fold formed subsequent to the formation of a thrust ramp, resulting in a modified fold geometry (Fig. 1c). Although not explicitly presented as a kinematic model, their fig. 3 (Fig. 1c) can be viewed as the sequential development of a fault-propagation fold and shares most of the characteristics outlined immediately above.

Wickham (1995) considered fault-propagation folds to be a subset of fault displacement–gradient folds in which fault propagation and fault slip do not necessarily occur contemporaneously. For example, a fold in the hanging wall of a thrust ramp may change shape if there is a progressive increase in the displacement while fault length remains constant (Wickham, 1995). Folding precedes faulting during the early development of break-thrust folds (Fischer *et al.*, 1992) but folding and faulting may be synchronous during the final stages of deformation (Morley, 1994).

Rather than comparing fold shape and fault geometry, an alternative procedure for the analysis of fault–fold relations involves consideration of the displacement gradient along a fault surface and the relationship of fault displacement and fault length (Williams and Chapman, 1983; McNaught and Mitra, 1993), factors controlled by the mechanical properties of rocks (Walsh and

*Present address: Department of Geological & Environmental Sciences, Stanford University, Stanford, CA 94305, U.S.A.

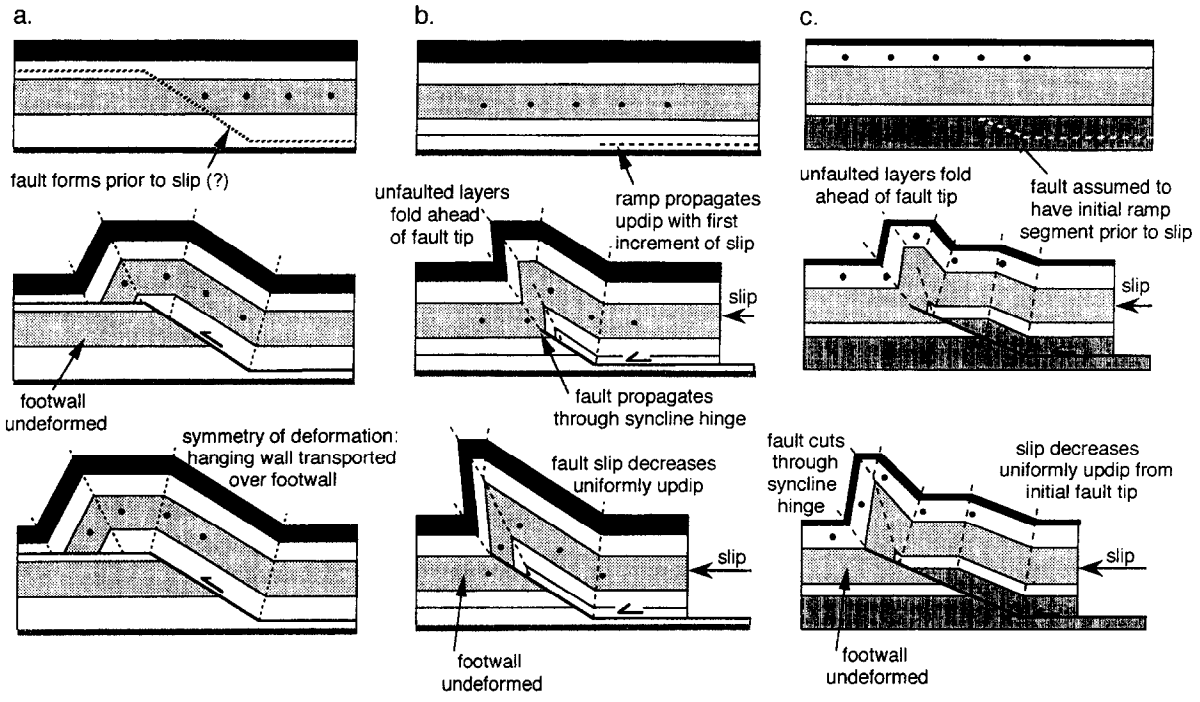

Fig. 1. Fault-related fold models: (a) fault-bend fold (Suppe, 1983); (b) fault-propagation fold (Suppe and Medwedeff, 1984, 1990); (c) fault-propagation fold (Chester and Chester, 1990).

Watterson, 1988; Cowie and Scholz, 1992; Gillespie *et al.*, 1992). Muraoka and Kamata (1983) proposed that fault propagation was rapid relative to fault slip in competent layers, thus, generating relatively long faults with little displacement. In contrast, they considered incompetent units to be 'strain absorbers' in which a fault would propagate slowly relative to slip. Armstrong and Bartley (1993) suggested that competent units may act as barriers to fault propagation, thus resulting in a progressive increase in the displacement gradient and the fault displacement:fault length ratio as slip continues. The degree of folding and associated deformation ahead of a fault tip increases where fault displacement is large relative to fault length (Chapman and Williams, 1984).

A common thread can be discerned between kinematic models of fault-related folds. Although they rarely acknowledge it, all kinematic models imply a specific relationship between the relative rates of fault propagation and fault slip. Faults with little concomitant folding form where fault length increases rapidly relative to fault displacement (Fig. 1a). The development of folds above fault tips will be favored when the rate of fault growth is low relative to the slip rate (Suppe and Medwedeff, 1984; Fig. 1b & c) or when the fault tip is pinned as fault slip increases (Wickham, 1995).

The rates of fault slip and propagation cannot be measured directly but two of the products of fault growth, fault length and fault displacement, may be determined. Displacement–distance diagrams (Fig. 2) illustrate the relationship between fault length (distance from the fault tip) and fault displacement and can be used to compare natural structures to kinematic models (Kattenhorn and McConnell, 1993). The displacement gradient (slope of the plotted line) is an indicator of the amount of deformation accommodated by mechanisms other than fault slip (Chapman and Williams, 1984). Steep lines are indicative of loss of displacement, as shortening is transferred to folds (Figs 2 & 3b) or when folding occurs as a result of a change in fault geometry (Fig. 3a). Slopes of zero represent portions of the fault

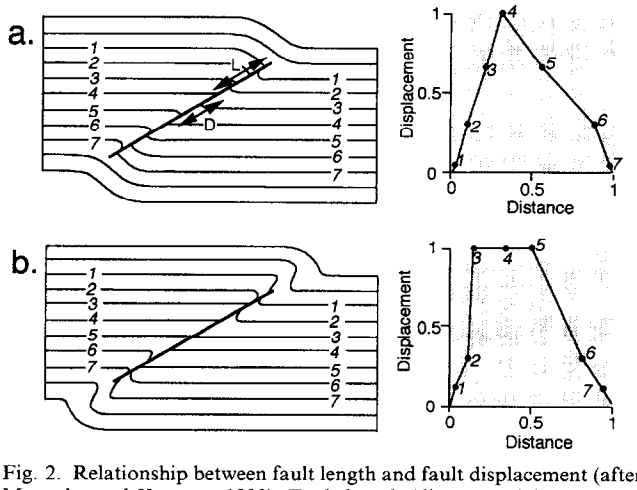

Fig. 2. Relationship between fault length and fault displacement (after Muraoka and Kamata, 1983). Fault length (distance, *L*) is measured from a reference point (here taken as the upper fault tip) to a layer in the hanging wall of the fault. Displacement (*D*) is measured parallel to the fault between the same layer in the hanging wall and footwall. Displacement–distance graphs are normalized to maximum values. (a) Displacement decreases up- and down-dip from a central maximum to generate a *C*-type (cone-shaped) profile. (b) Displacement is constant in layers 3, 4 and 5, to generate an *M*-type (mesa-shaped) profile.

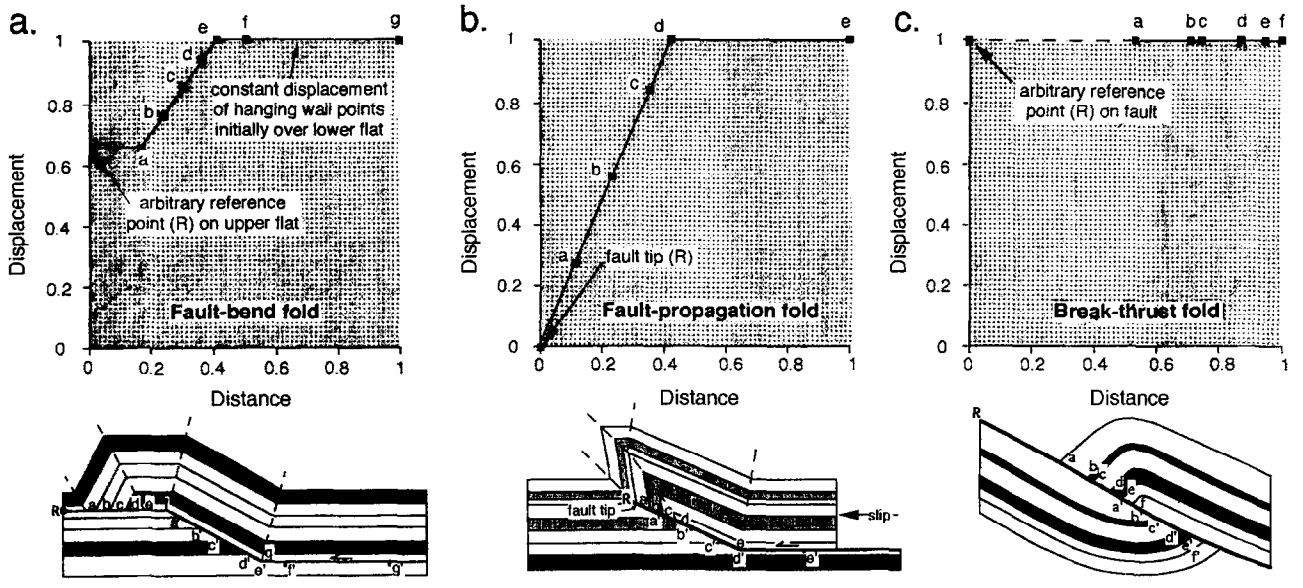

Fig. 3. Displacement–distance graphs for conventional models of fault-related folds. (a) Fault-bend folds (Suppe, 1983) display a sloping line for the hanging wall ramp, but show horizontal lines for upper and lower flats. Points a–e are bed cut-offs but points f and g lie above the lower flat and corresponding points below the flat would not be identifiable in natural structures. (b) Fault-propagation folds (Suppe and Medwedeff, 1984, 1990) display a sloping line for the beds above the ramp and a horizontal line for points above the lower flat where displacement is assumed to remain constant. Points a–d are bed cut-offs but point e was originally located above the lower flat and a corresponding point below the flat would not be identifiable in natural structures. (c) Break-thrust fold (Fischer *et al.*, 1992) displays constant displacement for bed cut-offs a–f.

where displacement remains uniform and may be indicative of fault segments that propagated with little associated folding (Figs 2b & 3a,b), or after folding occurred (Fig. 3c). The slope also provides an indication of the variation in displacement along the length of the fault. Positive slopes imply the fault loses displacement towards the fault tip or fault location used as a reference point (Figs 2 & 3), whereas, negative slopes indicate that slip diminishes with increasing distance from the tip. A displacement–distance diagram for a fault-bend fold has horizontal segments (uniform displacement) where the fault lies below hanging wall flats, has a steep slope (decreasing slip) for the portion of the fault beneath the hanging wall ramp (Fig. 3a), and the plot does not pass through the origin as the fault tip is not observed. In contrast, an equivalent diagram for a fault-propagation fold begins at the origin (fault tip) and has only one horizontal segment (Fig. 3b). In cases where faulting followed folding, there may be no discernible change in displacement across the fold (Fig. 3c). The plots illustrated in Fig. 3 are idealized. Using only data for ramp cut-offs would yield similar plots for fault-bend and fault-propagation folds which would then only be discernible by fold geometry. Both plots would yield positive slopes indicative of faults with uniform displacement gradients.

The majority of kinematic models predict that fold shape is dependent upon fault angle. However, individual fold geometries may be explained by several fault–fold configurations (Marshak and Woodward, 1988) or by more than one kinematic history (Morley, 1994). Furthermore, components of some natural structures may be absent from kinematic models. For example, footwall deformation is not observed in some models but is commonly associated with thrust faults (Protzman and Mitra, 1990; Evans and Neves, 1992; Watkinson, 1993; Spang, 1995) and aftershocks have been recorded from the footwalls of active faults (King and Yielding, 1984; Vita-Finzi and King, 1985).

Kinematic models typically display thrust ramps that propagate upwards from a bedding-parallel fault (Boyer and Elliot, 1982). However, thrust faults that lose displacement both up-dip and down-dip were recorded by Pfiffner (1985), Ellis and Dunlap (1988), and Ramsay (1992). Such variations in the mode of fault evolution will have consequences for fold growth. For example, Ellis and Dunlap (1988) documented examples of thrust faults with variations of displacement in which maxima were attributed to sites of fault nucleation and minima to points of fault coalescence. Eisenstadt and De Paor (1987) suggested thrust faults nucleate as ramps in competent units and propagate up- and down-dip to coalesce with bedding-parallel fault surfaces.

First-order fault-related folds in fold-and-thrust belts typically involve a 1–2 km thick section of sedimentary rocks (Fox, 1959; Perry, 1978; Kulander and Dean, 1986). The scale of these structures makes it difficult to view them in their entirety at the Earth's surface and the resolution of subsurface data sets is seldom sufficient to define the details of fault–fold relations. Furthermore, the cumulative deformation associated with thrust systems is often too complex to decipher the earliest stages of the structural evolution. Consequently, we investigated fault–fold relations in small-displacement, outcrop-scale, fault-related folds from the Valley and

Ridge province of the Appalachian fold-and-thrust belt. Such features can be described in their entirety and are free from overprinting by later deformation. Serra (1977) described several thrust faults at a similar scale in a study of deformation at thrust ramps. This paper expands Serra's analysis to include the nature of folding adjacent to the fault ramp. Examination of outcrop-scale structures in the Valley and Ridge province revealed that few of these fault-related folds match predictions of geometric and/or kinematic models, although elements of the models are present in several folds (McConnell and Kattenhorn, 1993).

OUTCROP-SCALE STRUCTURES

Eagle Rock, VA

Several fault–fold structures crop out in Silurian clastic rocks in roadcuts along US 220 and VA 43 near Eagle Rock, western Virginia (Fig. 4). The roadcuts are oriented approximately perpendicular to strike of both beds and faults and present cross-sectional views of fault–fold relations (Fig. 4b) in steeply inclined beds. Striations on fault surfaces are parallel to dip. Three structures are described here as Eagle Rock 1, 2, and 3 (Fig. 4b). Photographs of Eagle Rock 2 and 3 show the outcrops as they appear in the field but structures have been rotated in line drawings so that beds are subhorizontal with youngest units at the top of the drawing. The terms footwall and hanging wall are defined with reference to the line drawings. We make no assumptions about the orientation of the rocks during deformation.

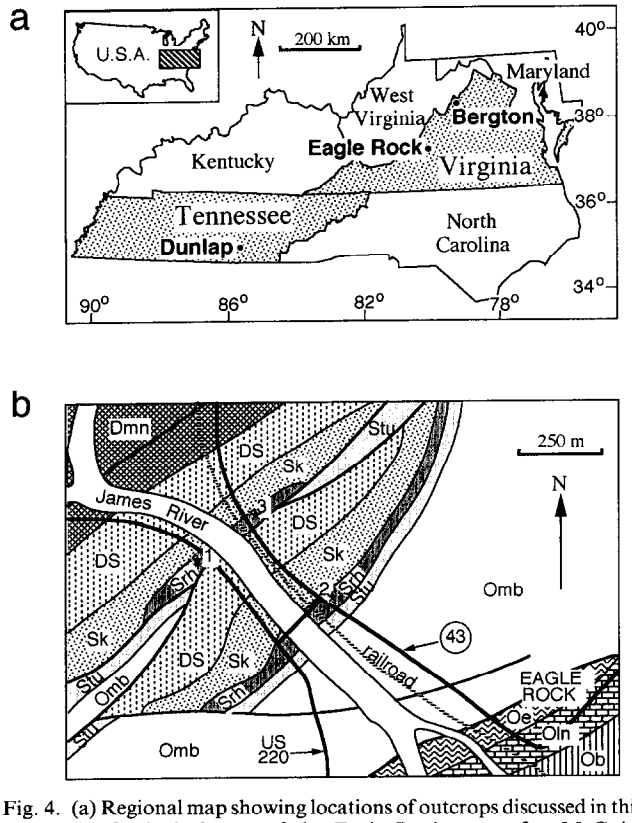

Fig. 4. (a) Regional map showing locations of outcrops discussed in this paper. (b) Geological map of the Eagle Rock area, after McGuire (1970). Numbered stars show locations of features Eagle Rock 1, 2, and 3. Thick black lines are faults. Abbreviations are: Dmn = Millboro and Needmore Shales; DS = Lower Devonian–upper Silurian undifferentiated rocks; Sk = Keefer Fm.; Srh = Rose Hill Fm.; Stu = Tuscarora Fm.; Omb = Martinsburg Fm.; Oe = Edinburg Fm. (Chambersburg Gp.); Oln = Lincolnshire Fm. and New Market Limestone; Ob = Beekmantown Fm.

Eagle Rock 1 has been described elsewhere (Kattenhorn and McConnell, 1994) and consists of steeply inclined (overturned) sandstone and shale beds offset by several small faults (Fig. 5). Layers offset by fault 1 (Fig. 5) are folded and form a hanging wall anticline and footwall syncline. The fault ramp cuts layering and has an upper and lower flat parallel to bedding. Several beds in the footwall adjacent to the ramp are shortened by folding (B–G). The equivalent units in the hanging wall are offset on the ramp but only beds F–I exhibit significant folding.

A contrasting deformation style is observed locally in a thin (8 cm) sandstone layer (bed M, Fig. 5) sandwiched between shale layers. Bed M is imbricated by more than 20 thrust faults that typically (but not exclusively) have the same sense of offset as faults 1 and 2 (Kattenhorn and McConnell, 1994). Displacement on fault 1 decreases up- and down-section from a maximum in bed G (Fig. 5). Maximum displacement on fault 2 occurs adjacent to the upper cut off of bed L (Fig. 5).

Three fault-related folds crop out at Eagle Rock 2 just outside the city limit of Eagle Rock (Figs 4b & 6). These structures contain elements that are consistent with fault-propagation folds (Figs 1b, c, 6, 7 & 8a) and fault-bend folds (Figs 1a, 6 & 8b). However, in these examples, folding is predominantly in the footwall, unlike conventional model predictions. The uppermost fold (Eagle Rock 2a, Figs 6 & 7) is offset by a ramp that cuts through the steep limb of the fold. Layers on both sides of the fault are folded and deformation in the hanging wall and footwall is complicated by several minor faults. Fold shape changes both up-section and down-section from the ramp as shortening is accommodated by the formation of a duplex in the hanging wall and by secondary faulting in the footwall. Displacement decreases down-section on the ramp from a maximum in bed J to zero at the base of bed D. The structure has several elements in common with an inverted Suppe and Medwedeff (1990) fault-propagation fold (Figs 1a, 6 & 7)

The lower thrust ramp in bed J in Eagle Rock 2b (Figs 6 & 8a) loses displacement down-section into an anticline. The hanging of the ramp exhibits little deformation. The ramp makes an angle of 22° relative to bedding but the distribution of displacement cannot be determined as the fault offsets a single bed. The geometry of the footwall syncline immediately adjacent to the fault tip is similar to an inverted version of the Chester and Chester (1990) fault-propagation fold model (Figs 1c & 8a).

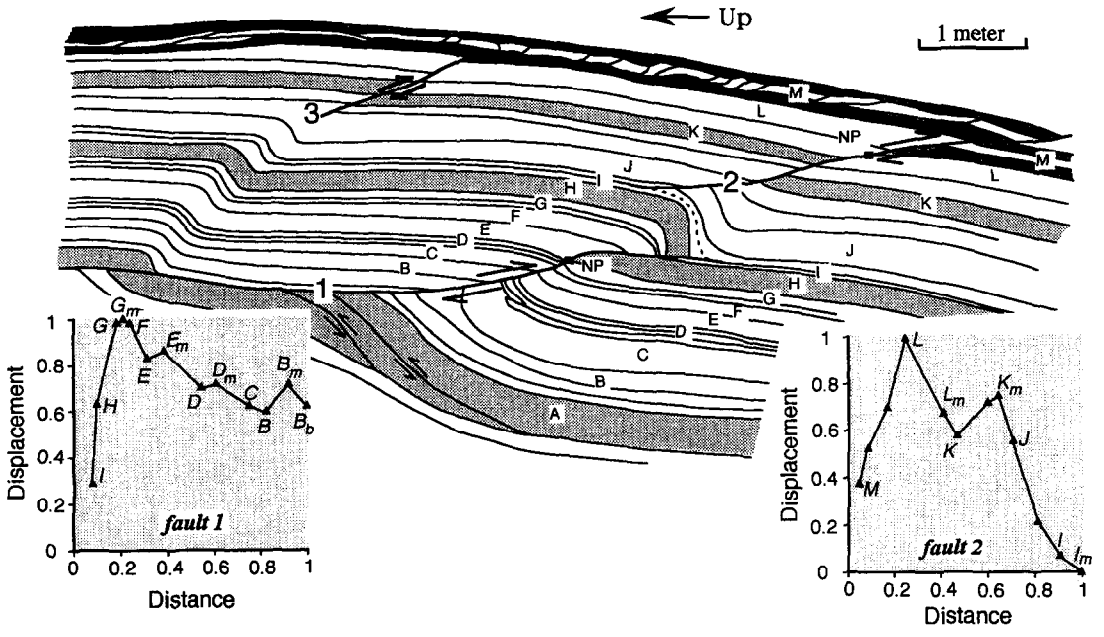

Fig. 5. Eagle Rock 1. Line drawing rotated so bedding is horizontal. NP = interpreted nucleation point with respect to the footwall. Displacement–distance diagrams for faults 1 and 2 are inset. Beds are labeled from A to M from oldest to youngest. Bed labels refer to the tops of beds unless otherwise indicated with a subscript b (base) or m (middle).

The ramp for the lowermost fault (Eagle Rock 2c) makes an angle of 15–20° with bedding-parallel fault segments (Figs 6 & 8b). Unlike other fault-related folds at this location, the hanging wall ramp overlies a footwall flat. This geometry is typically associated with fault-bend folds. However, this structure differs from a typical fault-bend fold as the footwall is folded and displacement decreases both up-dip and down-dip from a central point on the ramp (Fig. 8b).

Eagle Rock 3 (Figs 4b, 9 & 10a) contains syncline and anticline axial surfaces that intersect the fault at the tip and on the ramp, respectively, as predicted by fault-propagation fold models (Suppe and Medwedeff, 1984; Chester and Chester, 1990). Displacement on the fault diminishes rapidly as the fault passes from sandstone layers into thinly interbedded shales and siltstones. Fault slip is distributed on several splays and backthrusts making it impossible to create a displacement–distance diagram. Bedding plane slip, minor folding, and cataclastic flow within shale beds are common and resulted in bedding thickness variations (Fig. 9).

Bergton, VA

A double fault–fold structure crops out in Devonian (Chemung Group?) rocks along county road 820, off state route 259, near Bergton, Virginia (Fig. 4). Deformation occurs between two en échelon thrust faults in an outcrop of predominantly sub-horizontal sandstones, siltstones and shales (Figs 10b & 11). A fold pair is located adjacent to the fault tips in the zone of fault overlap. Displacement decreases towards the tips of both faults (Fig. 11). The lower fault is folded, presumably because of displacement on the upper fault.

Dunlap, TN

Several authors (Suppe, 1985; Chester and Chester, 1990; Mitra, 1990) have cited a fault-related fold (Fig. 12a) along state route 8, north of Dunlap, Tennessee (Fig. 4a), to illustrate contrasting models of fault-propagation folding (Benner and McConnell, 1995). The structure consists of a thrust-cored anticline in sub-horizontal Pennsylvanian Gizzard Group siltstones and sandstones in which the thrust ramp loses displacement upwards into a fold. Suppe (1985) interpreted folding to begin in the hanging wall when the ramp cut up-section from a detachment horizon. Chester and Chester (1990) noted that the lower layers in the hanging wall were not folded and suggested that the thrust ramp initially propagated without associated folding. Mitra (1990) described the structure as a fault-propagation fold that was later translated on a thrust which transported the syncline hinge in the hanging wall. Thrust faults of similar scale and orientation are present elsewhere in the roadcut (Wojtal, 1986) but few exhibit associated folding (Fig. 12b). Many of these faults continue below road level and thus their geometries and displacement distributions cannot be uniquely constrained. However, some other fault-related structures are also present and can be examined in their entirety (Figs 12c, d & 13).

The structure here labeled Dunlap 1 (Figs 12c & 13a) is located near the southern end of the roadcut. A thick sandstone bed (H, Fig. 13a) is offset by a fault that loses

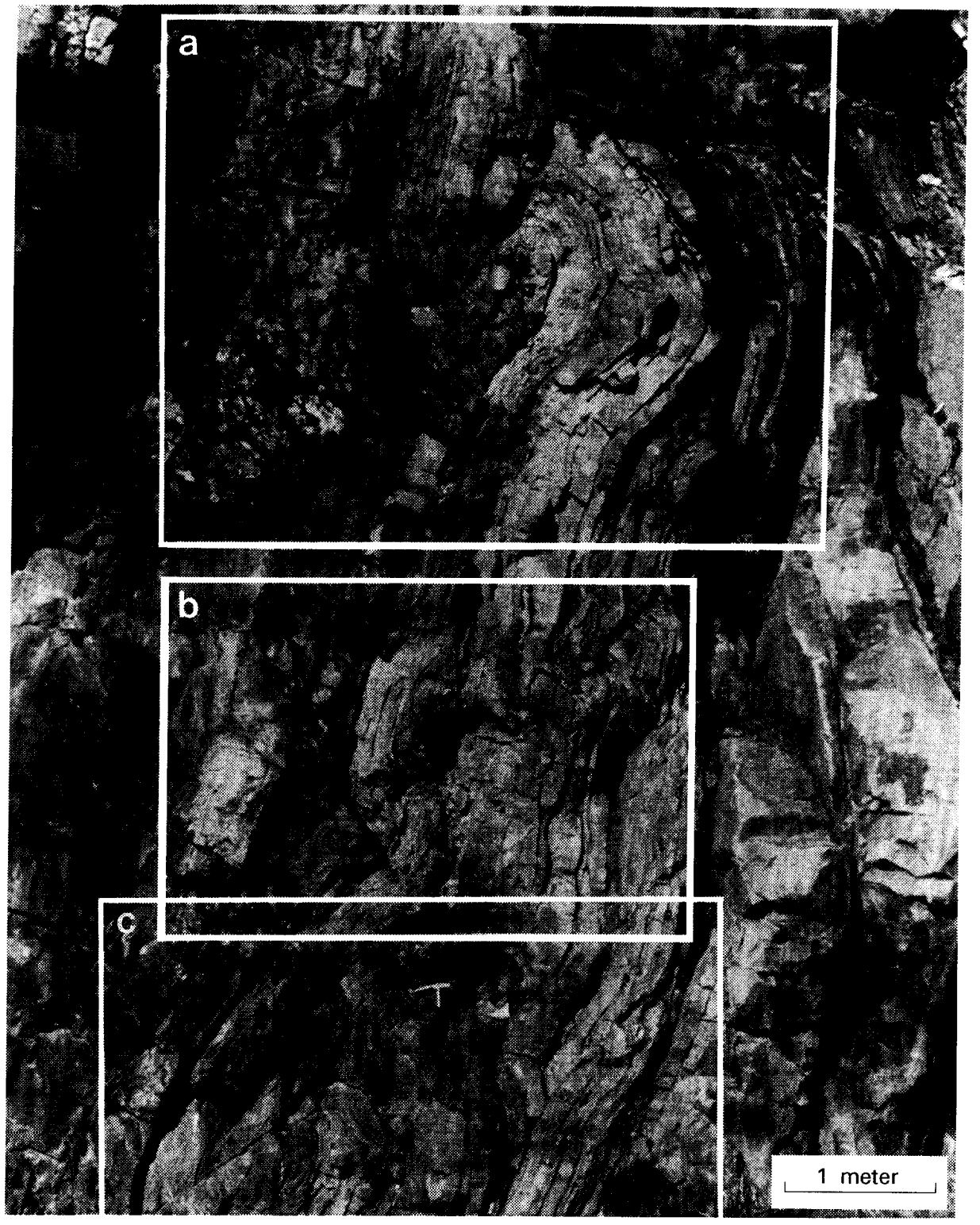

Fig. 6. Eagle Rock 2. Photograph of three fault-related folds at Eagle Rock 2 (Fig. 4b), view is to the northeast. Areas outlined by white boxes refer to line drawings in Fig. 7 (box a), Fig. 8(a) (box b), and Fig. 8(b) (box c).

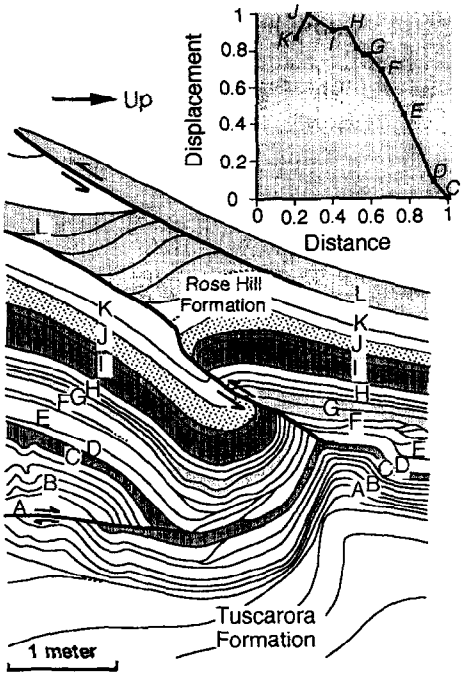

Fig. 7. Line drawing of Eagle Rock 2a. The figure has been rotated clockwise. Bedding thickness changes in the Tuscarora Formation are primary. The inset displacement–distance diagram illustrates that displacement decreases down-section into the footwall syncline.

displacement up-dip and down-dip. The overlying units exhibit thickness changes adjacent to the fault whereas the underlying layers were folded to form a footwall syncline (Fig. 13a). Dunlap 2 involves thrust faults of similar length to Dunlap 1 (Fig. 12c & d). However, displacement on these en échelon thrust ramps is much less and there is relatively little associated folding (Fig. 13c).

DISCUSSION

A key observation from the outcrop-scale structures is that thrust ramps lost displacement both up- and down-section (Figs 5–8 & 11–13). Corollaries of these observations were that footwall folds are often present and that ramps may be connected with upper and/or lower flats.

The decrease in displacement both up- and down-section from a point near the center of the fault (Figs 5, 11 & 13) or down-section from the top of a fault ramp (Figs 7 & 11) is interpreted to indicate that fault ramps may propagate down-section. Footwall synclines and hanging wall anticlines would form where folding precedes the propagating fault tip. This conceptual model (Fig. 14) explains the existence of footwall folds while accounting for the distribution of slip along the fault. All of these structures contain both folded and unfolded rocks in the footwall. Therefore, interpretation of the fault–fold configuration may depend upon the level of exposure (Fig. 14).

Several of the faults illustrated here lose displacement down-section into folds (Figs 7, 8a, 11 & 13a) generating

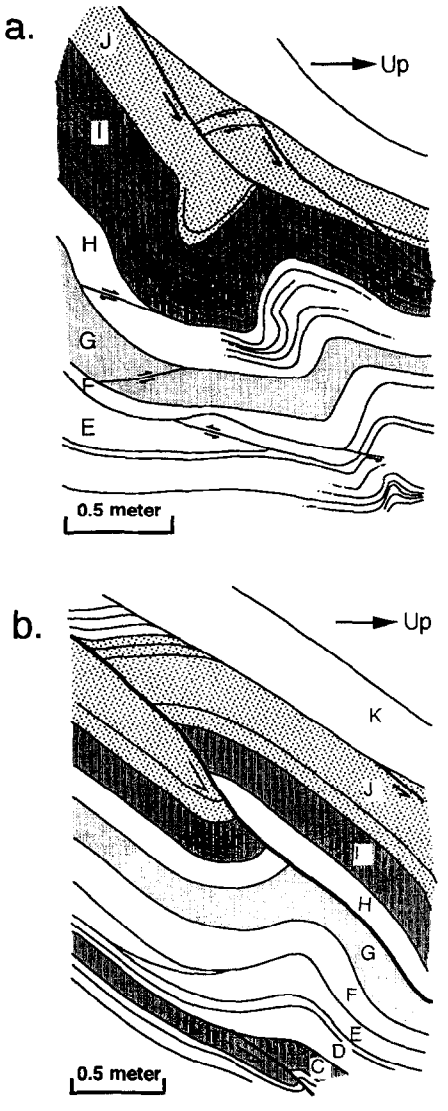

Fig. 8. Line drawings of Eagle Rock 2b and 2c. The figures have been rotated clockwise. (a) Eagle Rock 2b; (b) Eagle Rock 2c.

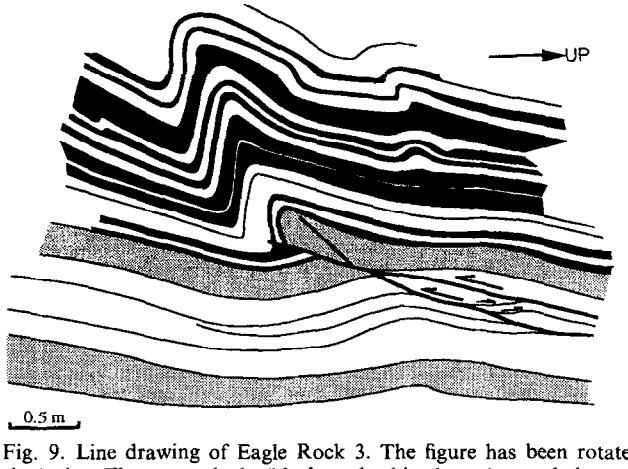

Fig. 9. Line drawing of Eagle Rock 3. The figure has been rotated clockwise. The upper beds (black and white layers) are shales and siltstones, the stipple pattern indicates sandstone beds.

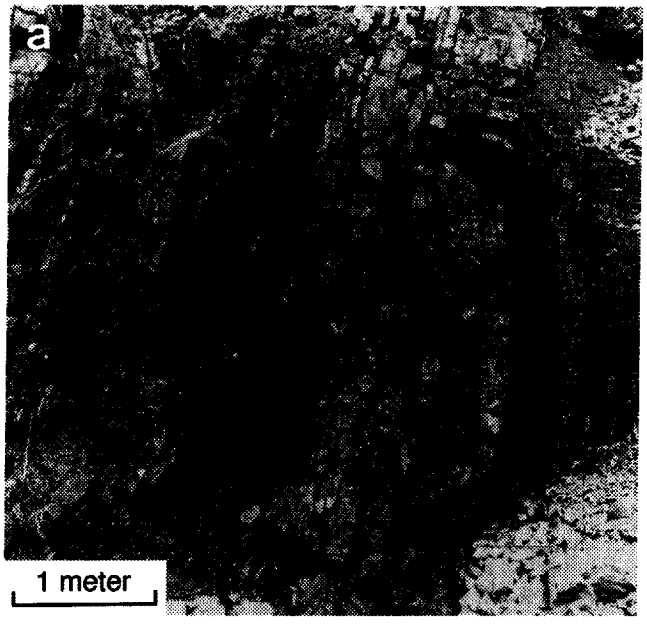

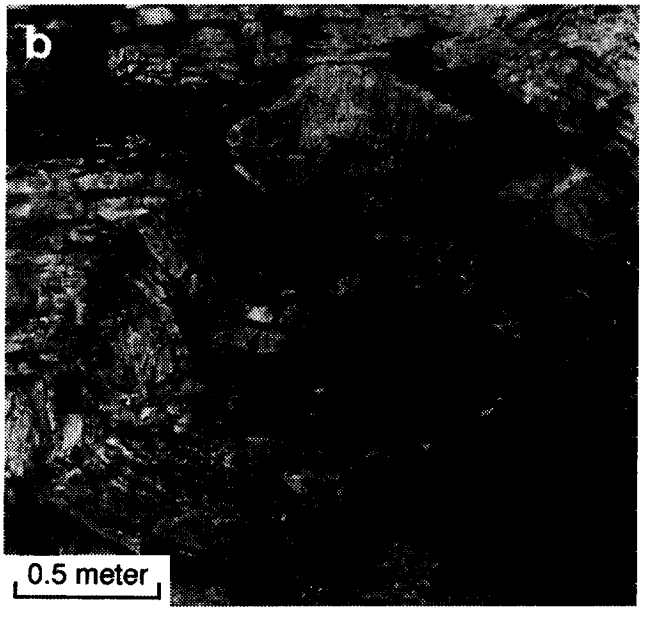

Fig. 10. Photographs of fault-related folds at Eagle Rock 3 and Bergton. (a) Eagle Rock 3 in outcrop position. (b) Close up of fault overlap at Bergton (see Fig. 11).

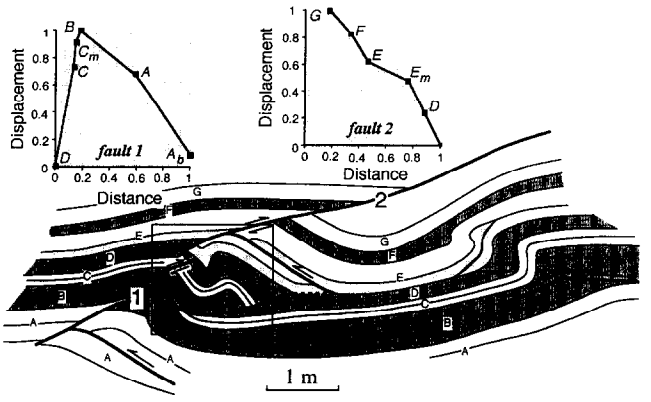

Fig. 11. Line drawing of fault-related folding near Bergton. Dark bands represent thinly-bedded units. Area outlined by box is illustrated in Fig. 10(b). Insets show displacement–distance graphs for faults 1 and 2. Bed labels refer to the tops of beds unless otherwise indicated with a subscript b (base) or m (middle).

fold geometries that have several features in common with inverted fault-propagation folds (Fig. 1b & c). The first-order similarity between fold geometries suggests that the folds form on the side of the fault that is displaced in the direction of fault propagation, but that the fault may propagate down-dip in a direction opposite to that typically displayed in models. The central fault-related fold at Eagle Rock 2 (Figs 6 & 8a) resembles the fold style of the Chester and Chester (1990) model (Fig. 1c). An inverted version of this model contains an additional fold panel that is absent in Eagle Rock 2b (Figs 1c & 8a). This additional segment may have been eradicated as displacement increased on the fault while the fault tip was pinned (Fig. 15; see also Armstrong and Bartley, 1993).

Some footwall folds may be accounted for as abandoned hanging wall structures (Mitra, 1990; Suppe and Medwedeff, 1990) or by folding preceding faulting (Fischer *et al.*, 1992). However, these models do not explain the contemporaneous faulting and footwall folding suggested by the displacement distributions of the natural structures described above. Cone-shaped (*C*-type) displacement–distance profiles (Fig. 2; Muraoka and Kamata, 1983) are generated by faults that nucleate at a central point and subsequently propagate up- and down-section. A nucleation point is represented by the peak of a displacement–distance diagram (for example, L in fault 2 graph, Fig. 5; J, Fig. 7), whereas troughs may indicated points were fault segments coalesced (for example K in fault 2 graph, Fig. 5; K in Fig. 13b; Ellis and Dunlap, 1988).

Physical and conceptual models (Dixon and Tirrul, 1991; Fischer *et al.*, 1992; Ramsay, 1992) have suggested that folding may precede faulting. However, in the examples presented here, folding is typically least developed adjacent to the point of maximum displacement (Figs 5, 7 & 13) and is therefore interpreted to have played a minor role prior to fault development.

It is inadvisable to directly extrapolate observations of small-displacement, outcrop structures to the scale of fold-and-thrust belts. The complex character of the mechanical stratigraphy, greater displacement on faults, increased importance of body forces, and the presence of an overlying free surface would influence the relationship between faulting and folding in ways that would not be replicated at the outcrop-scale. However, structures of up to 3 orders of magnitude larger are interpreted to have similar displacement distributions (Fox, 1959; Ellis and Dunlap, 1988; Morley, 1994). In addition, aftershocks located in the footwalls of active thrusts illustrate that footwall deformation occurs on much larger structures than the faulted-folds described herein (King and Yielding, 1984).

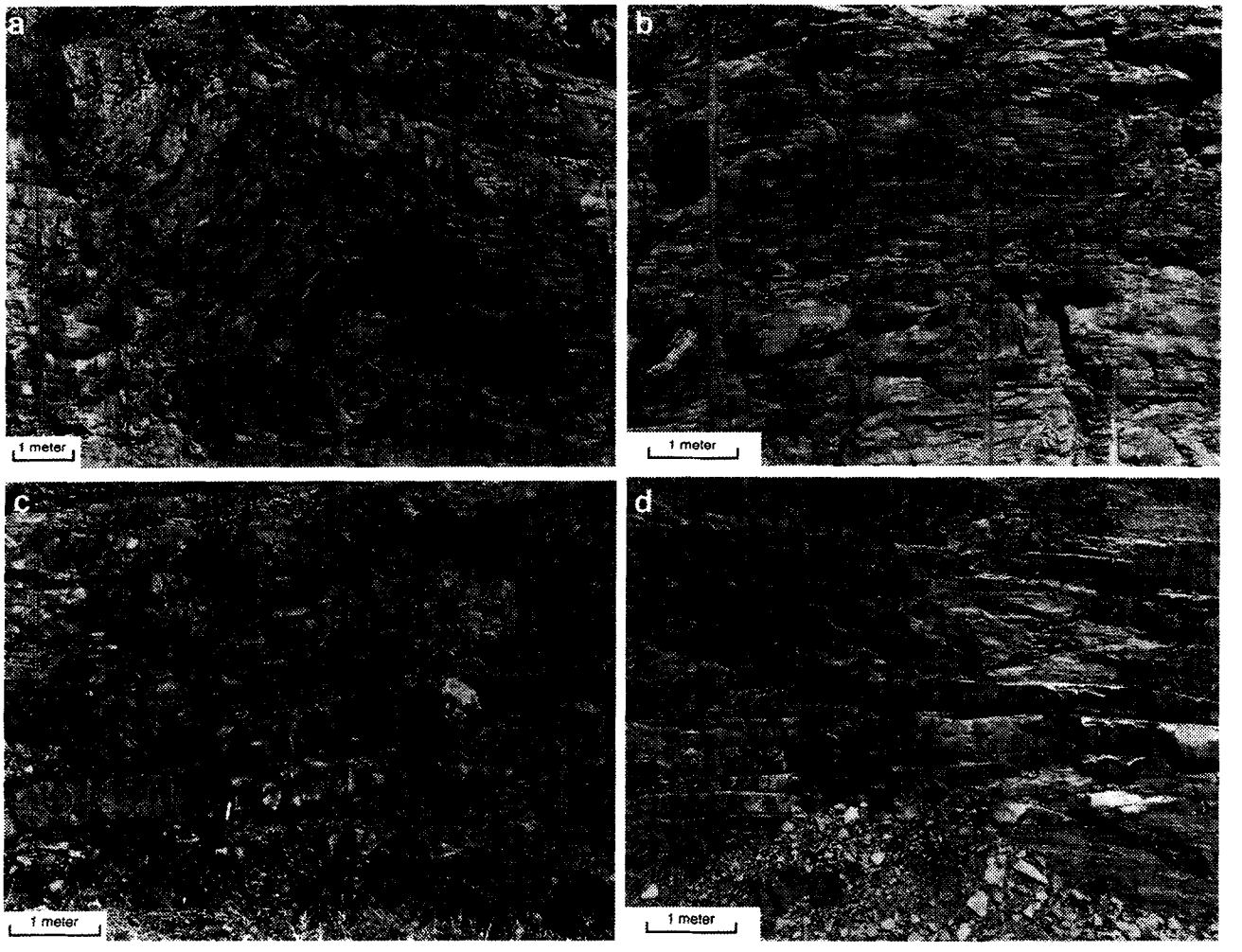

Fig. 12. Photographs of outcrop-scale thrust faults and associated structures in Pennsylvanian Gizzard Group rocks near Dunlap, Tennessee. Black bars are 1 m scales, black arrows show location of fault planes. (a) Thrust-cored fold-pair; (b) thrust fault with minimal displacement and no folding; (c) Dunlap 1, a thrust ramp offsets a thick sandstone bed (see Fig. 13a); (d) Dunlap 2, en échelon thrust ramps with little displacement (see Fig. 13c).

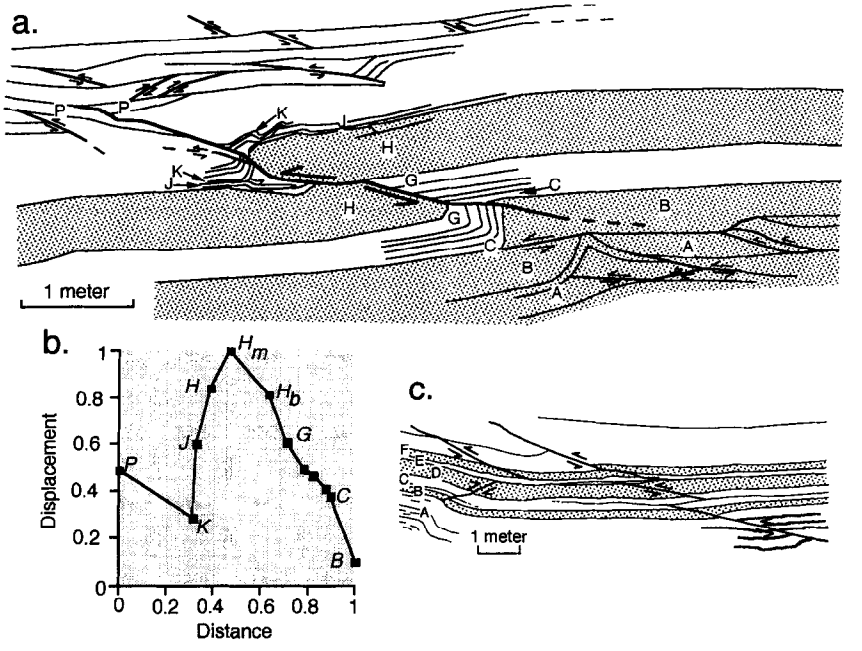

Fig. 13. Fault–fold relationships in Dunlap 1 and 2. (a) Line drawing of Dunlap 1 showing details of deformation associated with thrust fault. (b) Displacement–distance graph for Dunlap 1 (Fig. 12c). (c) Line drawing of Dunlap 2 (Fig. 12d) showing relative positions of three en échelon thrust ramps.

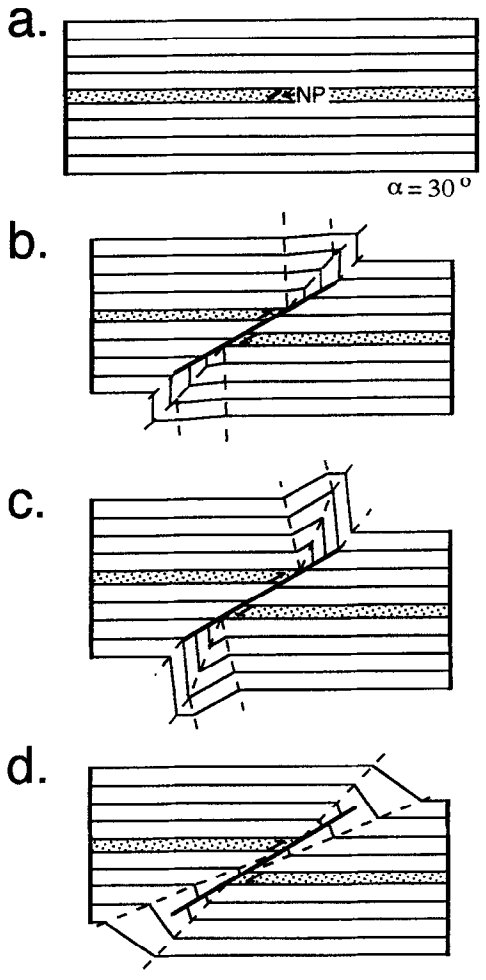

Fig. 14. Possible end-member fault-propagation fold styles produced by ramp-nucleated thrust faults of uniform dip. (a) Undeformed configuration showing nucleation point for the fault. (b) Fault-propagation fold configuration with backlimb not parallel to the ramp. (c) Fault-propagation fold with backlimb parallel to the ramp. (d) Fixed-hinge fault-propagation fold (after McConnell, 1994) with heterogeneous thickness changes in the forelimb.

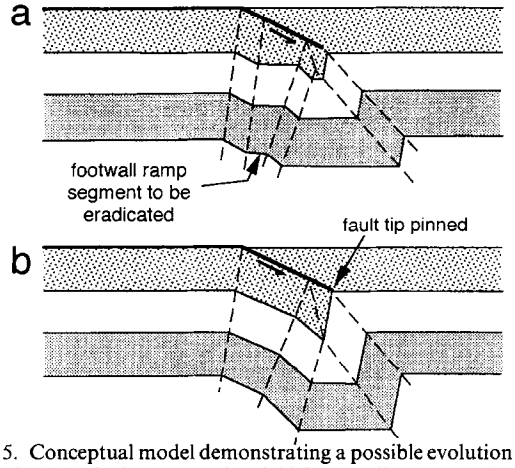

Fig. 15. Conceptual model demonstrating a possible evolution of Eagle Rock 2b. (a) A fault-propagation fold forms adjacent to a thrust ramp with a geometry similar to that predicted by Chester and Chester (1990). (b) The fault tip becomes pinned as displacement continues, eradicating the footwall ramp segment as the tip fold grows.

SUMMARY

Models of fault–fold evolution can provide sophisticated aids to the interpretation of structures in fold-and-thrust belts. Existing models are successful in predicting some of the fault–fold configurations observed in outcrop. However, these models imply specific sequences of deformation which do not account for some of the elements of deformation observed in simple, small displacement, outcrop-scale structures. Some of the deformation characteristics observed are:

(1) folding of hanging wall and/or footwall rocks;
(2) displacement increases both up- and down-dip on faults;
(3) fault ramps do not necessarily join a lower or upper detachment.

These observations are interpreted to suggest that current models may be adapted to incorporate ramp-nucleated faulted folds. These structures can potentially be distinguished from alternative fault–fold models by examining displacement–distance profiles. The existence of a lower flat does not rule out the ramp nucleation model, as it may also be compatible with situations where on-going fault growth involves the propagation of a ramp into a bedding-parallel flat.

Acknowledgements—Acknowledgment is made to the Donors of the Petroleum Research Fund, administered by the American Chemical Society, for support of this research. Simon Kattenhorn received support from the American Association of Petroleum Geologists and Sigma Xi. Reviews by Wesley Wallace, Michael Ellis, and Donald Fisher helped improve the paper.

REFERENCES

Armstrong, P. A. and Bartley, J. M. (1993) Displacement and deformation associated with a lateral thrust termination, southern Golden Gate Range, southern Nevada, U.S.A. *Journal of Structural Geology* **15**, 721–735.

Benner, L. M. and McConnell, D. A. (1995) Comparison of outcrop-scale fault-propagation folds near Dunlap, Tennessee, to kinematic model predictions. *Geological Society of America Abstracts with Programs* **27**, 36.

Boyer, S. E. (1986) Styles of folding within thrust sheets: Examples from the Appalachians and the Rocky Mountains of the U.S.A. and Canada. *Journal of Structural Geology* **8**, 325–339.

Buyer, S. E. and Elliot, D. (1982) Thrust systems. *Bulletin of the American Association of Petroleum Geologists* **66**, 1196–1230.

Chapman, T. J. and Williams, G. D. (1984) Displacement–distance methods in the analysis of fold–thrust structures and linked fault systems. *Journal of the Geological Society, London* **141**, 121–128.

Chester, J. and Chester, F. (1990) Fault propagation folds above thrusts with constant dip. *Journal of Structural Geology* **12**, 903–910.

Cowie, P. A. and Scholz, C. H. (1992) Displacement–length scaling relationship for faults: Data synthesis and discussion. *Journal of Structural Geology* **14**, 1149–1156.

Dixon, J. M. and Tirrul, R. (1991) Centrifuge modeling of fold–thrust structures in a tripartitie stratigraphic succession. *Journal of Structural Geology* **13**, 3–20.

Eisenstadt, G. and De Paor, D. G. (1987) Alternative model of thrust-fault propagation. *Geology* **16**, 33–36.

Ellis, M. A. and Dunlap, W. J. (1988) Displacement variation along thrust faults: Implications for the development of large faults. *Journal of Structural Geology* **10**, 183–192.

Evans, J. P. and Neves, D. S. (1992) Footwall deformation along Willard thrust, Sevier orogenic belt: Implications for mechanisms, timing and kinematics. *Geological Society of America Bulletin* **104**, 516–527.

Fischer, M. P., Woodward, N. B. and Mitchell, M. M. (1992) The kinematics of break-thrust folds. *Journal of Structural Geology* **14**, 451–460.

Fox, F. G. (1959) Structure and accumulation of hydrocarbon in southern Foothills, Alberta, Canada. *Bulletin of the American Association of Petroleum Geologists* **43**, 992–1025.

Gillespie, P. A., Walsh, J. J. and Watterson, J. (1992) Limitations of dimension and displacement data from single faults and the consequences for data analysis and interpretation. *Journal of Structural Geology* **14**, 1157–1172.

Jamison, W. R. (1987) Geometric analysis of fold development in overthrust terranes. *Journal of Structural Geology* **9**, 207–219.

Kattenhorn, S. A. and McConnell, D. A. (1993) Displacement–distance diagrams applied to the analysis of fault-propagation folds. *Geological Society of America Abstracts with Programs* **25**, 170.

Kattenhorn, S. A. and McConnell, D. A. (1994) Analysis of outcrop-scale fault-related folds, Eagle Rock, Virginia. *Southeastern Geology* **34**, 79–88.

King, G. and Yielding, G. (1984) The evolution of a thrust fault system: processes of rupture initiation, propagation and termination in the 1980 El Asnam (Algeria) earthquake. *Geophysical Journal of the Royal Astronomical Society* **77**, 915–933.

Kulander, B. R. and Dean, S. L. (1986) Structure and tectonics of central and southern Appalachian Valley and Ridge and Plateau provinces, West Virginia and Virginia. *Bulletin of the American Association of Petroleum Geologists* **70**, 1674–1684.

Marshak, S. and Woodward, N. (1988) Introduction to cross-section balancing. In *Basic Methods of Structural Geology*, eds S. Marshak and G. Mitra, pp. 303–332. Prentice-Hall, Englewood Cliffs, New Jersey.

McConnell, D. A. (1994) Fixed-hinge, basement-involved fault-propagation folds, Wyoming. *Bulletin of the Geological Society of America* **106**, 1583–1593.

McConnell, D. A. and Kattenhorn, S. A. (1993) Comparison of natural, outcrop-scale, fault-bend and fault-propagation folds to predictions of kinematic models. *Geological Society of America Abstracts with Programs* **25**, 169.

McGuire, O. S. (1970) Geology of the Eagle Rock, Strom, Oriskany and Salisburg quadrangles, Virginia. *Virginia Division of Mining. Research Report of Investigation* **24**.

McNaught, M. A. and Mitra, G. (1993) A kinematic model for the origin of footwall synclines. *Journal of Structural Geology* **15**, 805–808.

Mitra, G., Hull, J. M., Yonkee, W. and Protzman, G. M. (1988) Comparison of mesoscopic and microscopic deformation styles in the Idaho–Wyoming thrust belt and Rocky Mountain foreland. In *Interaction of the Rocky Mountain Foreland and the Cordilleran Thrust Belt*, eds C. J. Schmidt and W. J. Perry, Jr, 171, 119–141. Memoirs of the Geological Society of America.

Mitra, S. (1990) Fault-propagation folds: Geometry, kinematic evolution, and hydrocarbon traps. *Bulletin of the American Association of Petroleum Geologists* **74**, 921–945.

Morley, C. K. (1994) Fold-generated imbricates: Examples from the Caledonides of southern Norway. *Journal of Structural Geology* **16**, 619–631.

Mount, V. S., Suppe, J. and Hook, S. C. (1989) A forward modeling strategy for balancing cross-sections. *Bulletin of the American Association of Petroleum Geologists* **74**, 521–531.

Muraoka, H. and Kamata, H. (1983) Displacement distribution along minor fault traces. *Journal of Structural Geology* **5**, 395–483.

Perry, W. J. (1978) Sequential deformation in the central Appalachians. *American Journal of Science* **278**, 518–542.

Pfiffner, O. A. (1985) Displacements along thrust faults. *Eclogae Geologicae Helvetiae* **78**, 313–333.

Protzman, G. M. and Mitra, G. (1990) Strain fabric associated with the Meade thrust sheet: implications for cross-section balancing. *Journal of Structural Geology* **12**, 403–417.

Ramsay, J. (1992) Some geometric problems of ramp-flat thrust models. In *Thrust Tectonics*, ed. K. McClay, pp. 191–200. Chapman and Hall, London.

Serra, S. (1977) Styles of deformation in the ramp regions of overthrust faults. Wyoming Geological Association 29th Annual Field Conference Guidebook, 487–498.

Spang, J. H. (1995) Self-similar models of synclines in the footwall of thrust faults. *Geological Society of America Abstracts with Programs* **27**, 89.

Suppe, J. (1983) Geometry and kinematics of fault-bend folding. *American Journal of Science* **283**, 684–721.

Suppe, J. (1985) *Principles of Structural Geology*. Prentice-Hall, Englewood Cliffs, New Jersey.

Suppe, J. and Medwedeff, D. A. (1984) Fault-propagation folding. *Geological Society of America Abstracts with Programs* **16**, 670.

Suppe, J. and Medwedeff, D. A. (1990) Geometry and kinematics of fault-propagation folding. *Eclogae Geologicae Helvetiae* **83**, 409–454.

Vita-Finzi, C. and King, G. (1985) The seismicity, geomorphology, and structural evolution of the Corinth area of Greece. *Philosophical Transactions of the Royal Society, London* **A314**, 379–407.

Walsh, J. J. and Watterson, J. (1988) Analysis of the relationship between displacements and dimensions of faults. *Journal of Structural Geology* **10**, 239–247.

Watkinson, A. J. (1993) A footwall system of faults associated with a foreland thrust in Montana. *Journal of Structural Geology* **15**, 335–342.

Wickham, J. (1995) Fault displacement–gradient folds and the structure at Lost Hills, California (U.S.A.). *Journal of Structural Geology* **17**, 1293–1302.

Williams, G. D. and Chapman, T. J. (1983) Strains developed in the hanging walls of thrusts due to their slip/propagation rate: A dislocation model. *Journal of Structural Geology* **6**, 563–571.

Wojtal, S. (1986) Deformation within foreland thrust sheets by populations of minor faults. *Journal of Structural Geology* **8**, 341–360.